LUND UNIVERSITY

Prepulse dependence of X-ray emission from plasmas created by IR femtosecond laser pulses on solids

Steingruber, J; Borgstrom, S; Starczewski, T; Litzén, Ulf

[Link to publication]

LETTER TO THE EDITOR

Prepulse dependence of X-ray emission from plasmas created by IR femtosecond laser pulses on solids

J Steingruber†, S Borgström†, T Starczewski† and U Litzén‡

† Division of Atomic Physics, Lund Institute of Technology, PO Box 118, S-22 100 Lund, Sweden
‡ Division of Atomic Spectroscopy, Lund University, S-22 100 Lund, Sweden

Abstract. We report a strong prepulse dependence of the emission of X-rays from plasmas created by 150 fs Ti:sapphire laser pulses on solids. The laser pulses were focused onto plane samples of aluminium and vanadium with a main pulse power density of about 2.5×10^{16} W cm^{-2}. By splitting off a portion of the main pulse we were able to generate a prepulse whose delay and intensity were variable relative to the main pulse. With no prepulse, very weak X-ray radiation from Al^{9+} and Al^{10+} was observed, whereas a prepulse to main pulse ratio of more than 0.1% and the prepulse preceding the main pulse by more than 2 ns produced up to 50 times stronger X-ray output.

When high-intensity, ultra-short laser pulses are focused onto solids, a dense plasma is formed and X-rays are produced [1–5]. Basic studies of femtosecond laser pulse interaction with aluminium have previously been reported [6–8]. The importance of a laser prepulse in increasing the XUV and X-ray yields is well known and has, to some extent, already been studied in the sub-picosecond region [4, 9–14]. The aim of this work was to study the possibility of generating coherent X-rays from high-intensity, ultra-short laser pulses.

In this paper we report that a commercial high-intensity, ultra-short-pulse laser system may have inherent prepulses which are important in the production of strong X-ray radiation. A saturable absorber which reduces the laser prepulses may also strongly reduce the laser-produced X-rays. We also report on a systematic study of the X-ray production with an added ultra-short prepulse, variable in time delay and energy. The X-ray emission was observed both spectrally and spatially resolved.

The laser system used in our experiments has been described elsewhere [15]. It is a commercial system based on the chirped-pulse amplification technique consisting of an argon-ion-pumped Ti:sapphire oscillator, a diffractive pulse stretcher, frequency-doubled Nd:YAG laser-pumped regenerative and final amplifiers, and a diffractive pulse compressor. The normal output pulses carry 150 mJ of energy in 150 fs (FWHM) at 800 nm at a repetition rate of 10 Hz. The beam diameter is about 40 mm. The laser system itself produces prepulses which are difficult to eliminate completely. These prepulses originate in the regenerative Ti:sapphire amplifier. An intracavity Pockels cell switches in a pulse from the 76 MHz oscillator pulse train by altering the polarization axis from vertical to horizontal. Another intracavity Pockels cell switches out the amplified pulse after 15 round trips. Due to leakage before the final pulse switch-out, a number of prepulses are generated. An additional extracavity Pockels cell suppresses the leakage.

The ratio of the prepulse energy to the main pulse energy was measured by inserting a rough surface into the laser beam and measuring the scattered light with a fast, biased photodiode. Both the prepulse and the main pulse energies were measured with the same instrumental pulse width using suitable neutral-density filters in front of the photodiode.

Our measurements show that during 'normal' laser operation the prepulse to main pulse ratio at the time of the experiment was of the order of 1×10^{-4}. The exact number and relative amplitudes of the prepulses in the train were dependent on the actual laser adjustment, but the most common configuration comprised three distinguishable prepulses with energies of the same order of magnitude. These prepulses are separated by 11 ns in time (the round-trip time of the regenerative amplifier) and the last of the prepulses also arrives 11 ns ahead of the main pulse.

Amplified spontaneous emission (ASE) is known to be a problem in other laser systems. Under normal operating conditions ASE of the laser lies below our detection limit of 1×10^{-7} of the main pulse power. For this reason no plasma formation due to ASE should be expected in our case.

All the experiments were carried out with the laser beam at normal incidence to a polished target surface. Two different focusing arrangements were tested: off-axis parabolic mirrors with focal lengths of 125 mm and 250 mm, and a plane-convex lens with a focal length of 300 mm. No significant difference between the spectra obtained with the lens and the mirror could be observed with the laser prepulses present. Consequently, most of our studies were performed with a lens, which was the easiest component to adjust. The spot diameter at the target was calculated to be about 50 μm.

To ensure good reproducibility, it was necessary to fabricate and position the target carefully. For every laser shot, the target was moved so that the target surface conditions would be constant. At the tightest focusing condition, the green light of the $\frac{1}{2}$-harmonic, attributed to two-plasmon decay [17], dominates the visual appearance of the plasma spark. The experimental set-up is shown in figure 1.

A small portion at the edge of the beam was allowed to travel a shorter distance through a system of smaller mirrors, thus arriving before the main pulse creating the so-
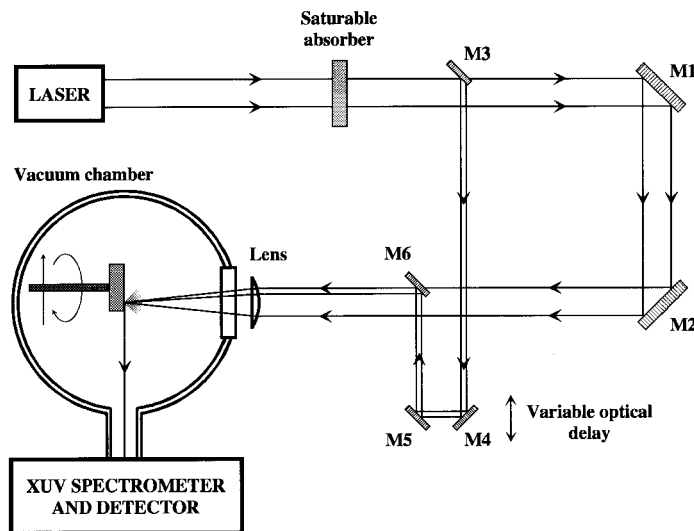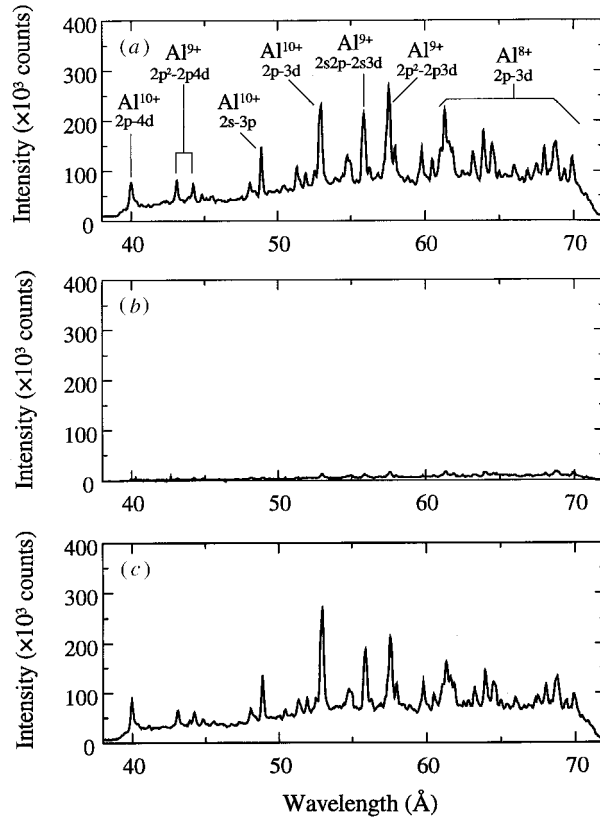
Figure 1. Experimental set-up.

Figure 2. X-ray spectra from laser-irradiated aluminium, (*a*) with laser prepulses; (*b*) without laser prepulses using a saturable absorber; (*c*) without laser prepulses, but with an artificial prepulse simulating the conditions in (*a*).

called artificial prepulse. The spatial overlap between this artificial prepulse and the main pulse was adjusted and checked with a telescope at a low laser power. The calculated spot sizes due to diffraction and spherical aberration of the artificial prepulse and the main pulse were found to be similar.

The spectra were obtained with a 2 m Schwob–Fraenkl grazing incidence spectrometer [18] with a 600l mm^{-1} grating. The detector was a micro-channel plate (MCP) with a CCD read-out. Examples of spectra, accumulated from 300 shots with a pulse energy of 80 mJ, are shown in figure 2. Figure 2(*a*) shows a 'normal' spectrum with the main laser pulse preceded by a train of three inherent prepulses, each about 4×10^{-4} of the main pulse energy and with no artificial prepulse. The spectrum in figure 2(*b*) was obtained after the beam had passed through a saturable absorber, which reduced the laser prepulses to about 3×10^{-7} of the main pulse. It is obvious that the X-ray production was much reduced. The saturable absorber consisted of a solution of the dye IR 140 in methanol, circulating between two anti-reflection coated glass plates of good optical quality. The glass plates had a thickness of 3 mm each and the dye film was 4 mm thick. The dye deteriorated when it was exposed to laser light and had to be renewed frequently. The main pulse was also absorbed in the dye to some extent. This was compensated for by adjusting the laser power so that the energy of the laser at the target was kept at a constant value.

The spectrum in figure 2(*c*) was obtained after removing inherent prepulses from the laser pulse and adding an artificial prepulse. The time delay was 11 ns and the artificial prepulse to the main pulse ratio was 4×10^{-4}. The spectra in figures 2(*a*) and (*c*) are thus comparable, showing that both the saturable absorber and the generation of an artificial prepulse work well.

Several spectra similar to those in figure 2 were collected under various prepulse conditions, also for the wider spectral region ranging from 20 Å to 300 Å. Figure 2 shows that the introduction of a prepulse before a clean laser pulse significantly increased the X-ray signal from higher ionization stages (e.g. Al^{10+} and Al^{9+}) by a factor of up to 50. On the other hand, it was observed that the X-rays from lower ionization stages (e.g. Al^{3+} at 160 Å and Al^{4+} at 120 Å) only increased by a factor of 3. Similar results were obtained with vanadium as the target material.

We also studied the X-ray emission spectrally integrated but spatially resolved. The laser-produced plasma was observed through a pinhole with a diameter of 15 μm, situated 130 mm away from the plasma, at an angle of 90 to the laser beam. To absorb the long-wavelength radiation a 100 nm thick aluminium filter was placed behind the pinhole. A back-illuminated CCD chip (512 $\times$ 512 pixels, area 13 mm $\times$ 13 mm) was placed 630 mm from the pinhole to detect the X-rays. Typical images are shown in figure 3, illustrating the effect of the prepulse. The image size corresponds to the estimated focal spot size of 50 μm. With this arrangement, a systematic study of the variation in X-ray emission with various artificial prepulses added to a clean main pulse was performed. The inherent laser prepulses were suppressed by the saturable absorber. Using an optical delay line (see figure 1), the artificial prepulse could arrive between 0 and 12 ns ahead of the main pulse. Also, the energy of the prepulse could be easily varied up to 3% of the main pulse energy by aperturing the beam. In all cases, the main pulse energy was kept at 80 mJ, corresponding
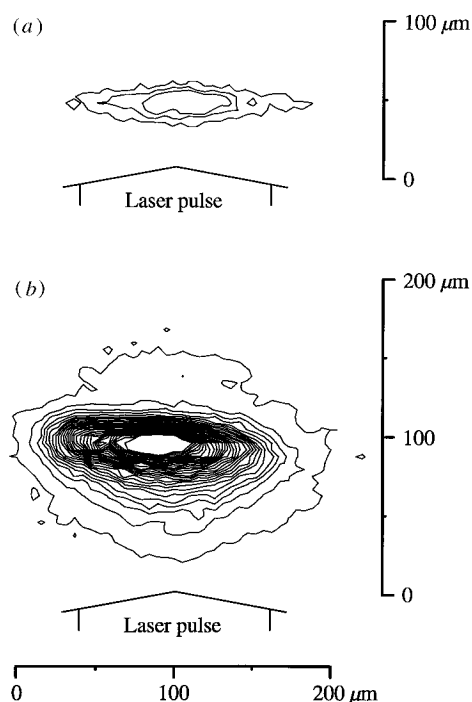

Figure 3. Contour plots of the CCD image of the laser-produced plasma obtained through a pinhole and an aluminium filter. The count difference between adjacent lines is approximately the same in both plots, (*a*) no laser prepulse, artificial prepulse ratio of 1.0×10^{-3}; (*b*) no laser prepulse, artificial prepulse ratio of 1.3×10^{-2}.
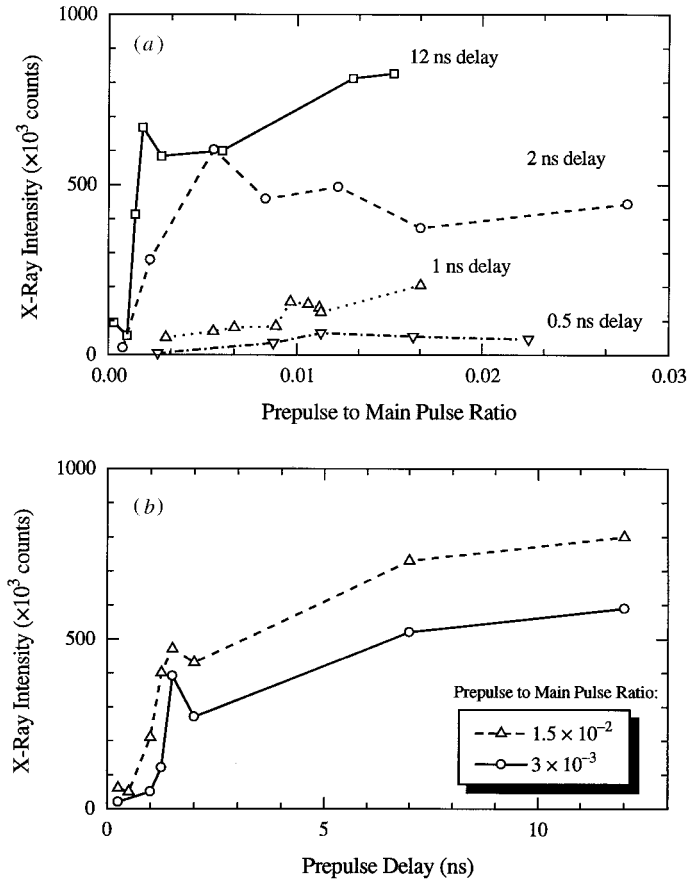
Figure 4. Spectrally and spatially integrated X-ray yields from a laser-irradiated aluminium target, (*a*) versus the prepulse to main pulse ratio (for different time delays); (*b*) versus the time delay between the prepulse and the main pulse (for two different prepulse intensities).

to 2.5×10^{16} W cm^{-2}.

Figure 4(*a*) shows the total, spatially integrated X-ray signal versus the prepulse to main pulse ratio at different time delays. Figure 4(*b*) shows the total X-ray signal versus the time delay for two different prepulse to main pulse ratios. All curves in figure 4(*a*) seem to start around 10^{13} W cm^{-2}, the intensity needed for plasma formation [19], corresponding in our case to a prepulse to main pulse ratio of 4×10^{-4}.

A theoretical understanding of the experimental results was obtained by using a one-dimensional hydrodynamic code, HYDRO [20]. Using the code, we calculated the temperatures and densities of ions and electrons in the plasma created by the prepulse and the main pulse. These quantities were calculated as a function of time and of the distance from the target surface. The only absorption mechanism used in the calculation was the inverse bremsstrahlung absorption.

For a prepulse intensity of 10^{14} W cm^{-2}, the maximum temperature of the prepulse plasma given by the code was 14 eV. Although only the inverse bremsstrahlung absorption was taken into account, the calculated electron temperatures agreed within 20% of the measured values [6] for intensities between 5×10^{13} and 10^{15} W cm^{-2}. After the main
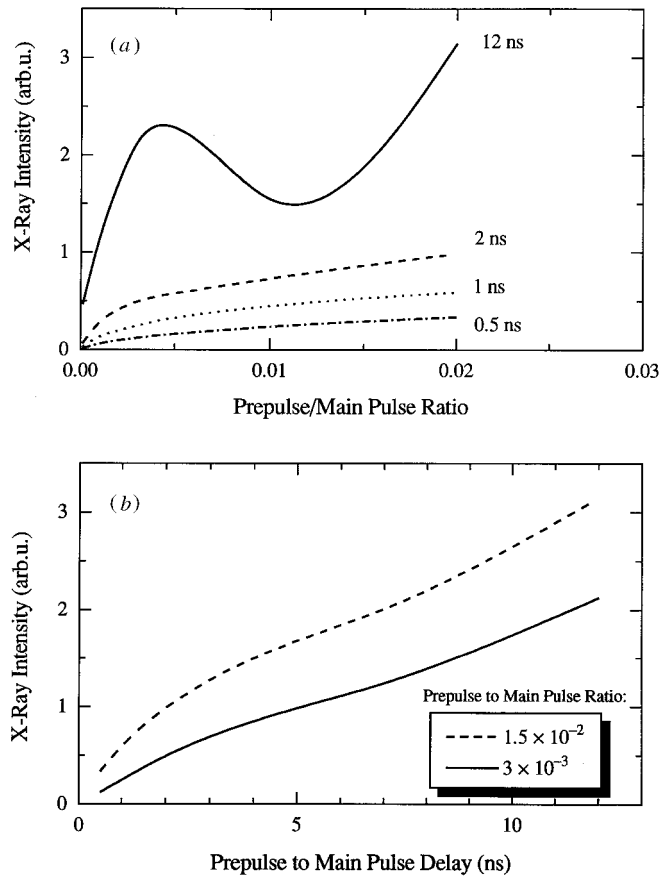
Figure 5. Calculations corresponding to the experimental curves of figure 4.

pulse had hit the prepulse plasma, the maximum electron temperature increased to 1000 eV.

The time- and space-integrated X-ray emissions were calculated with a local thermal Equilibrium (LTE) model including the strongest lines of H-like, He-like and Li-like ions, bremsstrahlung and self-absorption using the results from the hydrodynamic code. The assumption of LTE was justified because at the electron density of 1.2×10^{21} cm^{-3} (the critical density) and a temperature of 1000 eV, the electron–ion collision time is about 30 fs, a time much shorter than the laser pulse duration. The dominating part of the X-ray emission emanated from the hot, dense part of the plasma.

The results showing the time- and space-integrated X-ray emissions with different prepulse conditions are shown in figure 5. This diagram should be compared with figure 4. Generally, the X-ray intensity increases with increasing time delay between the prepulse and the main pulse. It also increases with increasing prepulse intensity. This is readily understood because a longer time delay or a more intense prepulse produces a more extended plasma with more ions, promoting the absorption of the main pulse, leading to a more effective X-ray source.

The experimental data show a similar behaviour as a function of the prepulse delay and the prepulse intensity. For low prepulse intensities and short delays the X-ray signal was very sensitive to changes of the preplasma parameters. There is also a peak after the steep

rise of the signal in both figure 4(a) and (b). These peaks were significant and reproducible and indicate that the X-ray yield depends on the spatial extension of the preplasma.

The calculated data increase monotonously and show a peak only for the longest delay of 12 ns. In addition, that peak is much broader than the experimental one. The reason for the peak is that for a long delay and a high prepulse ratio ($>1\%$), the critical surface of the preformed plasma is relatively far away from the solid surface ($\sim$10 μm). In this case, the main pulse can no longer heat the high-density region of the target surface efficiently and the signal drops. At even higher prepulse ratios, the signal again increases because of the larger preplasma volume, as mentioned before. For shorter delays ($<$ 2 ns) and lower prepulse ratios ($<1\%$), the distance from the critical surface to the solid is less than 2 μm leading to more efficient heating of the high-density region close to the solid. In fact, the calculation shows that, in this case, the X-ray signal is dominated by bremsstrahlung which is proportional to $N_e^2\sqrt{T_e}$, whereas for the 12 ns delay and a high prepulse, the X-ray radiation consists of equal parts of bremsstrahlung and line radiation.

We believe that a process similar to that described above may be responsible for the peaks we observed in our experiments. In the calculations, we only considered classical heat transport and absorption, which seem to explain the main features of the experimental results. However, more refined theories would be needed to account for the finer details and to achieve a more accurate description.

References

[1] Stearns D G, Landen O L, Campbell E M and Scofield J H 1988 *Phys. Rev.* A **37** 1684
[2] Wood II O R, Silfvast W T, Tom H W K, Knox W H, Fork R L, Brito-Cruz C H, Downer M C and Maloney P J 1988 *Appl. Phys. Lett.* **53** 654
[3] Zigler A, Burkhalter P G, Nagel D J, Boyer K, Luk T S, McPherson A, Solem J C and Rhodes C K 1991 *Appl. Phys. Lett.* **59** 777
[4] Kmetec J D, Gordon C L III, Macklin J J, Lemoff B E, Brown G S and Harris S E 1992 *Phys. Rev. Lett.* **68** 1527
[5] Herrlin K, Svahn G, Olsson C, Pettersson H, Tillman C, Persson A, Wahlström C G and Svanberg S 1993 *Radiology* **189** 65
[6] Milchberg H M, Freeman R R, Davey S C and More R M 1988 *Phys. Rev. Lett.* **61** 2364
[7] Wang X Y and Downer M C 1992 *Opt. Lett.* **17** 145
[8] Audebert P, Geindre J P, Rouse A, Fallies F, Gauthier J C, Mysyrowicz A, Grillon G and Antonetti A 1994 *J. Phys. B: At. Mol. Opt. Phys.* **27** 3303
[9] Cobble J A, Schappert G T, Jones L A, Taylor A J, Kyrala G A and Fulton R D 1991 *J. Appl. Phys.* **69** 3369
[10] Kühlke D, Herpers U and von der Linde D 1987 *Appl. Phys. Lett.* **50** 1785
[11] Murnane M M, Kapteyn H C and Falcone R W 1989 *Phys. Rev. Lett.* **62** 155
[12] Theobald W, Wülker C, Jasny J, Szatmari S, Schäfer F P and Bakos J S 1994 *Phys. Rev.* E **49** R4799
[13] Nam C H, Tighe W, Valeo E and Suckewer S 1990 *Appl. Phys.* B **50** 275
[14] Teubner U, Kühnle G and Schäfer F P 1992 *Appl. Phys.* B **54** 493
[15] Svanberg S, Larsson J, Persson A and Wahlström C G 1994 *Phys. Scr.* **49** 187
[16] Baldis H A, Campbell E M and Kruer W L 1991 *Handbook of Plasma Physics* vol 3 *Physics of Laser Plasma* ed A Rubenchik and S Witkowski (Amsterdam: North-Holland) pp 377–80
[17] Schwob J L, Wouters A W, Suckewer S and Finkenthal M 1987 *Rev. Sci. Instrum.* **58** 1601
[18] Vu B T V, Szoke A and Landen O L 1994 *Phys. Rev. Lett.* **72** 3823
[19] Schlegel T Max-Born Institute for Non-Linear Optics, Berlin, Germany